Journal of Catalysis 268 (2009) 201–208

Contents lists available at ScienceDirect

Journal of Catalysis

journal homepage: www.elsevier.com/locate/jcat

The effect of Co-promotion on MoS_2 catalysts for hydrodesulfurization of thiophene: A density functional study

Poul Georg Moses [a], Berit Hinnemann [b,*], Henrik Topsøe [b], Jens K. Nørskov [a]

[a] *Center for Atomic-Scale Design (CAMD), Department of Physics, Building 307, Technical University of Denmark, DK-2800 Kgs. Lyngby, Denmark*
[b] *Haldor Topsøe A/S, Nymøllevej 55, DK-2800 Kgs. Lyngby, Denmark*

ARTICLE INFO

Article history:
Received 10 July 2009
Revised 14 September 2009
Accepted 22 September 2009
Available online 23 October 2009

Keywords:
Hydrodesulfurization
Hydrogenation
DFT
Co–Mo–S
Brim sites
Thiophene
Reaction Mechanism
DDS
HYD

ABSTRACT

We present density functional theory (DFT) calculations of the hydrogenation (HYD) and direct desulfurization (DDS) pathways of thiophene hydrodesulfurization (HDS) over cobalt-promoted MoS_2. We find that the Co–Mo–S edge in its equilibrium state under HDS conditions is reactive toward both hydrogenation and C–S bond scission without the initial creation of vacancies. This can be accomplished such that additional S is bound to the Co–Mo–S subsequent to C–S bond scission and then removed in the final reaction step. We find thus that coordinatively unsaturated sites (CUS) are present in the equilibrium structure, and at these sites HDS can take place without sulfur removal in the first step. No traditional vacancies are formed and the present mechanism is therefore very different from the previously proposed vacancy mechanisms requiring the initial creation of a sulfur vacancy for the reaction to proceed. We find that Co-promotion decreases the barrier of hydrogenation reactions and active site regeneration but increases the barrier of C–S-scission reactions. The net result of Co promotion is found to be an increase in the hydrogenation activity and also of the relative importance of the DDS pathway. We compare our results to available experimental information and find a number of consistencies and parallels. Therefore, we can rationalize the promoting effect of Co such that at the Co–Mo–S edge, good hydrogenation properties are combined with the ability to bind additional sulfur upon C–S-scission. Finally, we propose that the interactions between the Co-promoted S-edge and the non-promoted Mo-edge may play a role in the hydrogenation pathway.

1. Introduction

MoS_2-based catalysts are widely used as hydrodesulfurization (HDS) catalysts and the need to optimize these catalyst is driven by both the need to process heavier feeds and the increasing demand for ultra clean diesel products. Typically, Co- or Ni-promoted MoS_2 is used for industrial HDS catalysts, since promotion of MoS_2 with Co or Ni increases the activity of the catalyst [1]. In this work, we focus on Co-promotion, and the structure responsible for catalytic activity in Co-promoted catalysts is the Co–Mo–S-type structure [2], which consists of MoS_2 particles in which Mo-edge atoms are substituted by Co or Ni. The Co–Mo–S structure was initially identified by using a series of *in situ* techniques [1]; and recent joint theoretical and experimental investigations have revealed that Co substitutes Mo atoms at the $(\bar{1}010)$ edge of MoS_2 [3–8]. This edge is commonly denoted as the S-edge, whereas the other low-index $(10\bar{1}0)$ edge is denoted as the Mo-edge. Despite the increased understanding of the Co–Mo–S structure, very little is known about the nature of the active site and the reaction mechanism of HDS over Co–Mo–S catalysts. Furthermore, there is still much debate on the effect of promotion with regard to the relative increase in hydrogenation and C–S-scission activity [9–15] and the resistivity toward inhibitors such as H_2S [9,11,16].

For a long time it has been a common belief that the catalytic activity of HDS is related to its ability to form sulfur vacancies, i.e., coordinatively unsaturated sites (CUS) at which sulfur can be bound subsequent to carbon–sulfur bond scission [1,17,18]. The present results show that this simple picture has to be modified somewhat. Therefore, this concept warrants further discussion. A natural starting point for each edge structure is its stoichiometric termination. However, this may not be the structure dominating under different experimental or reaction conditions, but such structures can be determined from DFT-based phase diagrams [6,18–21]. These phase diagrams reveal a large variety of structures with different sulfur and hydrogen coverages depending on temperature and H_2 and H_2S partial pressures. It is interesting that we found [22] that in several cases the equilibrium structures "as is" are reactive toward hydrogenation and/or sulfur scission. For example, we found in our previous study that the relevant Mo-edge structure can adsorb thiophene and catalyze HDS on unpromoted MoS_2. In other cases, sulfur has to be removed first for the

---

* Corresponding author. Fax: +45 4527 2999.
E-mail address: behi@topsoe.dk (B. Hinnemann).

0021-9517/$ - see front matter © 2009 Elsevier Inc. All rights reserved.
doi:10.1016/j.jcat.2009.09.016

edge to be reactive at all, as was calculated for the S-edge in our previous study of MoS_2 [22,23]. For the unpromoted Mo-edge, we would thus consider this edge to be “born with sulfur vacancies”, which means that sulfur vacancies are already present in the equilibrium structure. In contrast, for the unpromoted S-edge, sulfur vacancies have to be created first. For promoted structures, Byskov et al. showed some years ago that the introduction of Co and Ni to the MoS_2 edges increases the tendency to form vacancies [4]. In contrast, the incorporation of Fe, which is known not to be an efficient promoter, did not decrease vacancy formation energy [4]. More recently, scanning tunneling microscopy (STM) [24] revealed that MoS_2 nano-clusters have bright brim structures (the so-called brim sites) which were subsequently identified by DFT to be formed by metallic edges states [25] and combined STM and DFT studies showed that these sites may play a role in adsorption, hydrogenation, and C–S-scission [26,27]. These brim sites may be reactive without removal of sulfur in the first step, i.e. they may already contain sulfur vacancies in their equilibrium structure. In the present paper, we demonstrate a similar reaction mechanism for the Co–Mo–S edge. In its equilibrium structure, the sulfur coordination number is four, but additional sulfur atoms can be bound easily subsequent to C–S-scission.

For the case of unpromoted MoS_2 catalysts, we have recently performed DFT calculations of the complete thiophene HDS pathway [22,23]. In the present paper, we extend these mechanistic studies to Co-promoted systems and present the pathways for thiophene HDS over Co–Mo–S structures. In Section 3.1, we present the equilibrium edge configuration of the Co-promoted S-edge under typical HDS conditions and introduce the different investigated elementary reactions. In Sections 3.2 and 3.3, we investigate the hydrogenation (HYD) and direct desulfurization (DDS) pathways, with the two pathways being defined in the same way as in Ref. [22]. Specifically, the DDS pathway is defined as the pathway which is initiated by an initial addition of an hydrogen atom to carbon 2 forming 2-hydro-thiophene-3-yl which reacts further by direct C–S-scission. In the HYD pathway,thiophene is hydrogenated such that 2,5-dihydrothiophene is formed prior to the initial C–S bond scission. In Section 3.4 we compare the results for Co–Mo–S for the two pathways to those for the unpromoted MoS_2 catalyst. In Section 3.5, we discuss the overall effect of promotion.

2. Computational details

An infinite stripe model, which had previously been used successfully to model MoS_2-based systems [4,19,22,28], is used to investigate the edges of Co–Mo–S. The infinite stripe exposes both the Mo-edge and the S-edge. We use a unit cell consisting of 4 Mo atoms in the x-direction and 4 Mo atoms in the y-direction. The stripes are separated by 14.8 Å in the z-direction and 9 Å in the y-direction. This model represents MoS_2 structures with no support interactions and can be regarded as a model for Type II structures found in present-day high activity commercial catalysts [29–31]. The plane-wave density functional theory code DACAPO [32,33] is used to perform the DFT calculations. The Brillouin zone is sampled using a Monkhorst–Pack k-point set [34] containing 4 k-points in the x-direction and 1 k-point in the y- and z-direction. The calculated equilibrium lattice constant of $a = 3.22$ Å compares well to the experimental lattice constant of 3.16 Å [35]. A plane-wave cutoff of 30 Rydberg and a density-wave cutoff of 45 Rydberg are employed using the double-grid technique [36]. Ultrasoft pseudopotentials are used except for sulfur, where a soft pseudopotential is employed [37,38]. A Fermi temperature of $k_BT = 0.1$ eV is used for all stripe calculations and energies are extrapolated to zero electronic temperature. The exchange correlation functional PW91 is used [39]. All calculations have been performed spin polarized, due to the presence of cobalt. The convergence criterion for the atomic relaxation is that the norm of the total force should be smaller than 0.15 eV/Å, which corresponds approximately to a maximum force below 0.05 eV/Å on one single atom. Fixed bond length filters and the nudged elastic band (NEB) method are used to find energy barriers [40] together with the adaptive nudged elastic band approach [41] and cubic spline fits to the energies and the forces. Furthermore, a fixed bond length filter and a transition state search algorithm have been used to check NEB transition states. The algorithm utilizes a quasi Newton algorithm and an approach similar to the one presented in [42] to follow the eigenvector corresponding to the lowest eigenvalue to the saddle point. Figures of atomic structures have been made using VMD [43].

All adsorption energies have, unless otherwise noted, been calculated using the equation:

$$E_{\mathrm{ad}} = E_{\mathrm{molecule+MoS_2}} - E_{\mathrm{MoS_2}} - E_{\mathrm{molecule}(g)}, \tag{1}$$

where $E_{\mathrm{molecule+MoS_2}}$ is the energy of the system with the molecule bound to the surface, $E_{\mathrm{MoS_2}}$ is the energy of the stripe, and $E_{\mathrm{molecule}(g)}$ is the energy of the molecule in vacuum. Molecules in vacuum have been calculated with the same setup as stripe calculations, except using a supercell which ensures at least 11 Å vacuum between neighboring molecules, a Fermi temperature of $k_BT = 0.01$ eV, gamma point sampling of the Brillouin zone, and a tighter force convergence criterion, which requires that the norm of the total force be smaller than 0.05 eV/Å.

3. Results

3.1. The active sites in equilibrium structures

We investigate the Co-promoted S-edge, since experiment and theory have found that Co atoms preferentially substitute Mo atoms at the S $(\bar{1}010)$ edge [3,5–8]. We focus on the fully promoted S-edge which in addition to providing insight into the fully promoted MoS_2 also provides a reference point for understanding partially substituted edges such as the structures proposed in reference [3,44,45] and observed for NiMoS [7]. We find that the Co–Mo–S edge at HDS conditions is covered with 50% S and 25% H (Fig. 1) using a thermodynamic model similar to the one described in Ref. [19]. Thus, compared to the fully sulfided S-edges the promoted edges are “born” with vacancy sites and we find that they are reactive toward thiophene without any prior removal of sulfur. The edge Co atoms are 4-fold coordinated to S. Thus, they have a lower coordination number than the edge Mo atoms at the corresponding unpromoted equilibrium S-edge, since at this edge Mo atoms are 6-fold coordinated to S. The Co–Mo–S preference for a lower S coordination number than MoS_2 can be understood as a result of the preferred valence state of Co(II) compared to Mo(IV), and thus at the same chemical potential of sulfur Co prefers a lower S coordination than Mo. Consequently, one can regard the Co–Mo–S equilibrium structure as having one sulfur vacancy per MoS_2 unit cell present. These findings are in good agreement with earlier DFT results [6,20] and with EXAFS experiments which determined the S coordination number to be substantially below 6 [46,47].

It is interesting to note that the HDS equilibrium edge is similar to the edge observed in STM experiments [7], except for the H coverage. STM provides very valuable atomic insight into the structure and reactivity of this edge. Usually, the STM experiments are performed at higher H_2S/H_2 ratios than those found under HDS conditions which give rise to the slightly different edge structures. However, DFT calculations carried out at both sets of conditions can link the STM experiments to real HDS conditions. In this

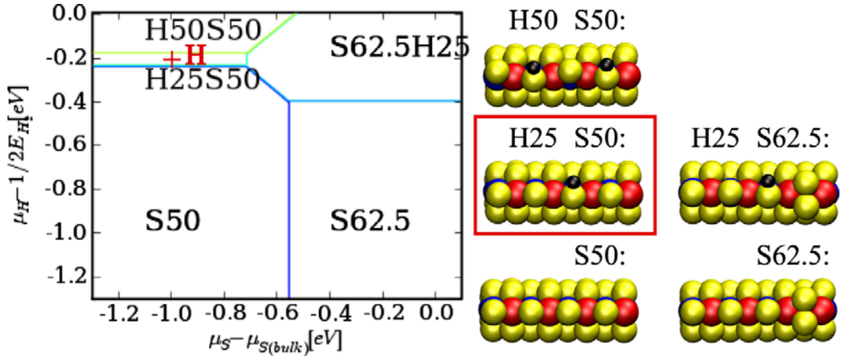

Fig. 1. Phase diagram of the S $(\bar{1}010)$ Co–Mo–S edge. (+H) mark the chemical potential at HDS condition ($P_{H_2} = 10$ bar, $P_{H_2}/P_{H_2S} = 100$ and $T = 650$ K). The stable edge configuration at HDS conditions is emphasized by a red square. (For interpretation of the references in colour in this figure legend, the reader is referred to the web version of this article.)

way, STM combined with DFT provides direct atomic insight into the edge present at HDS conditions.

The active site at the equilibrium edge can either be at one of the vacancies formed by Co-promotion or an additional S vacancy created in the equilibrium structure. However, creating this additional vacancy in the Co–Mo–S structure, i.e. removing a sulfur atom from the equilibrium structure, requires 1.8 eV (calculated as $\Delta E_{vac} = E_* + E_{H_2S(g)} - E_{H_2(g)} - E_{S-*}$) in good agreement with a recent study of HDS of DBT [48]. This value is even higher than that for the non-promoted equilibrium S-edge ($\Delta E_{vac} = 1.69$ eV) and renders the creation of these additional vacancies very unlikely. This indicates that the active sites at the Co–Mo–S $(\bar{1}010)$-edge are the vacancy sites created by Co-promotion and are present in the equilibrium edge structure.

The equilibrium Co–Mo–S edges have been observed to exhibit a bright brim right behind the edge with protrusions at the front row S atoms [7]. We denote these sites as "Co–Mo–S brim sites", since they are analogous to the Mo-edge brim sites. The Co–Mo–S brim sites have a coverage of one as they are present on the entire edge at equilibrium edge configuration.

We investigate both the HYD and the DDS pathways at the Co–Mo–S brim site using the same definition of the two different pathways as for MoS_2 [22]. We define the DDS as the pathway where the initial C–S scission takes place in the 2-hydro-thiophene-3-yl species formed after one hydrogen addition reaction. In the HYD pathway, the initial C–S scission takes place in dihydrothiophene after addition of two hydrogen atoms. We do not consider tetrahydrothiophene as an intermediate, because it is known that at HDS conditions hydrogenation of 2,5-dihydrothiophene is thermodynamically unfavored [1,49]. We assume that the second addition of a hydrogen atom, which hydrogenates 2-hydro-thiophene-3-yl into 2,5-dihydrothiophene as well as the reaction for the final S removal from cis-2-butenethiol have zero barrier, as we calculated a zero or close to zero barrier for these reactions on both the S- and Mo-edge of MoS_2 [22].

To find the reaction path, we investigate several adsorption configurations for all the intermediates. We only list the most relevant structures below and an overview of all the intermediates is provided in the Supplementary material. In Table 1, the HDS reactions at the Co–Mo–S brim site are summarized along with the non-promoted S-edge for comparison. To allow for easy comparison with the results for the unpromoted MoS_2 structures in Ref. [22], we use the same numbering of the reactions. Fig. 2a shows the contracted reaction path which has been constructed under the assumption that gas phase hydrogen is in equilibrium with surface hydrogen.

Until recently van der Waals (vdW) interactions have not been included in DFT: Recently, however, a new XC-functional which includes vdW interactions has been developed [50]. We have implemented this scheme in the grid-based real space projected augmented wave code GPAW [51,52] and applied it to adsorption on MoS_2 [52]. We find that the binding due to vdW interactions is considerable (−0.5 eV for thiophene on the MoS_2 basal plane), and thus the coverage of thiophene is likely to be higher than that we calculate here due to the absence of vdW interactions. Furthermore, in Ref. [52] we found a linear correlation between the number of main atoms and the vdW adsorption energy. For the present study, this means that the inclusion of vdW interactions in the reaction path energy diagram to a first approximation leads to a constant down shift of the entire reaction path by ~0.5 eV. However, the conclusions which are drawn in this work are based on the energy differences and will not be affected by vdW interactions.

3.2. HYD pathway

The HYD pathway shown in Fig. 2a is initiated by thiophene adsorption (reaction X in Table 1). The weakly bound thiophene (−0.1 eV) reacts further by addition of an hydrogen atom to carbon 2 to form 2-hydro-thiophene-3-yl (reaction I in Table 1) with a calculated barrier of 0.4 eV which is equal to the calculated energy change of the reaction. The second hydrogen addition reaction in which 2,5-dihydrothiophene is formed is assumed to be non-activated in accordance with the results from MoS_2 [22]. After the formation of 2,5-dihydrothiophene the HYD pathway proceeds by an initial C–S-scission reaction for which we find that the C–S bond can be broken without involving a H atom (reaction XIV in Table 1). The subsequent hydrogen addition reaction (reaction XV in Table 1) leads to the formation of cis-2-butenethiolate and has a barrier of 0.05 eV. The overall barrier of the initial C–S-scission reaction is 1.67 eV and is given by the activation energy of reaction XIV, because the activation energy of the subsequent hydrogen addition reaction (reaction XV) is negligible (0.05 eV). Reactions XIV and XV may therefore be contracted to reaction III in Table 1 with $E_a = 1.67$ eV and $\Delta E = -0.1$ eV. Reaction III is followed by a H transfer reaction (reaction IV in Table 1) which leads to cis-2-butenethiol with an activation energy of 1.0 eV. The final C–S scission reaction is assumed to be non-activated, justified by the 0.0 eV and 0.1 eV barriers at the non-promoted MoS_2 S-edge and Mo-edge, respectively.

The HYD pathway may also proceed via a different route after the C–S bond breaking in 2,5-dihydrothiophene (reaction XIV), since the second C–S bond can be broken directly without further hydrogen addition (reaction XVI), thereby forming *cis*-butadiene. The overall activation barrier for this pathway is given by the initial C–S-scission (reaction XIV) barrier of 1.67 eV, since the direct

Table 1
An overview of the reactions involved in HDS of thiophene over Co–Mo–S and the non-promoted S-edge including the activation barriers (E_a) and energy changes (ΔE) of the reactions. Non-promoted S-edge values are taken from Ref. [22].

Reaction		Co–Mo–S		S-edge	
		E_a (eV)	ΔE (eV)	E_a (eV)	ΔE (eV)
I	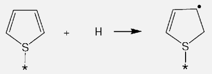	0.44	0.44	0.80	0.43
II	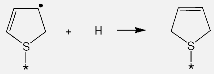	0.0[f]	−1.01	0.00	−1.02
III	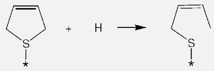	1.67[e]	−0.10	0.82	−0.78
IV	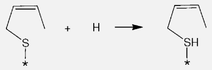	0.96	0.21	1.63	1.09
V	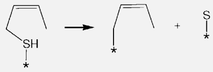	0.00[f]	−0.72	0.0	−0.66
VI		0.63	0.03	0.21	−1.11
VII	$2HS-*\rightarrow H_2S-*+S-*$	1.00[a]	−0.01	1.70[a]	1.57
VIII	$1/2H_{2(g)}+*\rightarrow H-*$		−0.24[b]		−0.57
IX	$H_2S_{(g)}+*\rightarrow H_2S-*$		−0.02[b]		−0.12
X	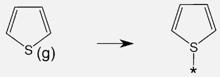		−0.07[c]		0.21
XI			−0.57[c]		−0.59
XII			−0.55[c]		−0.52
XIII	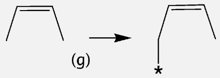		−0.03[d]		−0.05
XIV	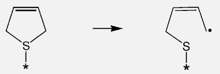	1.67	1.59		
XV	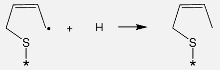	0.05	−1.69		
XVI	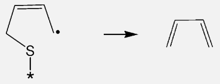	0.01	0.32		

[a] Calculated as $E_{VII}=\Delta E_1+E_2$, where ΔE_1 is the reaction energy of reaction 1: 2H–S (25% H and 50% S) + S(0% H and 62.5% S) + S–S (0% H and 62.5% S) → 2 (0% H and 50% S) + H–S–S (50% H and 62.5% S) + H–S (50% H and 62.5% S) and $E_2 = 0.54$ eV is the activation energy of reaction 2: H–S–S (50% H and 62.5% S) + H–S (50% H and 62.5% S) → H_2S–S (50% S).

[b] 50% S and 0% H.

[c] 50% S and 25% H.

[d] 62.5% S and 0% H.

[e] Proceeds in two steps, (1) S–C scission without involving H (reaction XIV), (2) hydrogenation (reaction XV). The overall activation energy is given by the E_a of step 1 due to the low barrier of step 2.

[f] The activation energy is assumed to be 0.00 eV which is justified by results on MoS_2 [22].

breaking of the second bond is non-activated (0.01 eV). Thus, sulfur can be removed without forming a thiolate. A detailed microkinetic model is needed to determine the relative importance of the two different HYD pathways. However, in both cases the highest barrier is the initial C–S-scission, indicating that the overall rate of the two HYD pathways will be similar. However, one could speculate that the pathway leading to *cis*-butadiene might be dominating due to the fact that this pathway does not involve hydrogen. Experimentally, it has been difficult to distinguish between the pathways, and this may be related to fast adsorption and further hydrogenation of butadiene. Perhaps, reaction studies on planar model systems may provide further detailed insight.

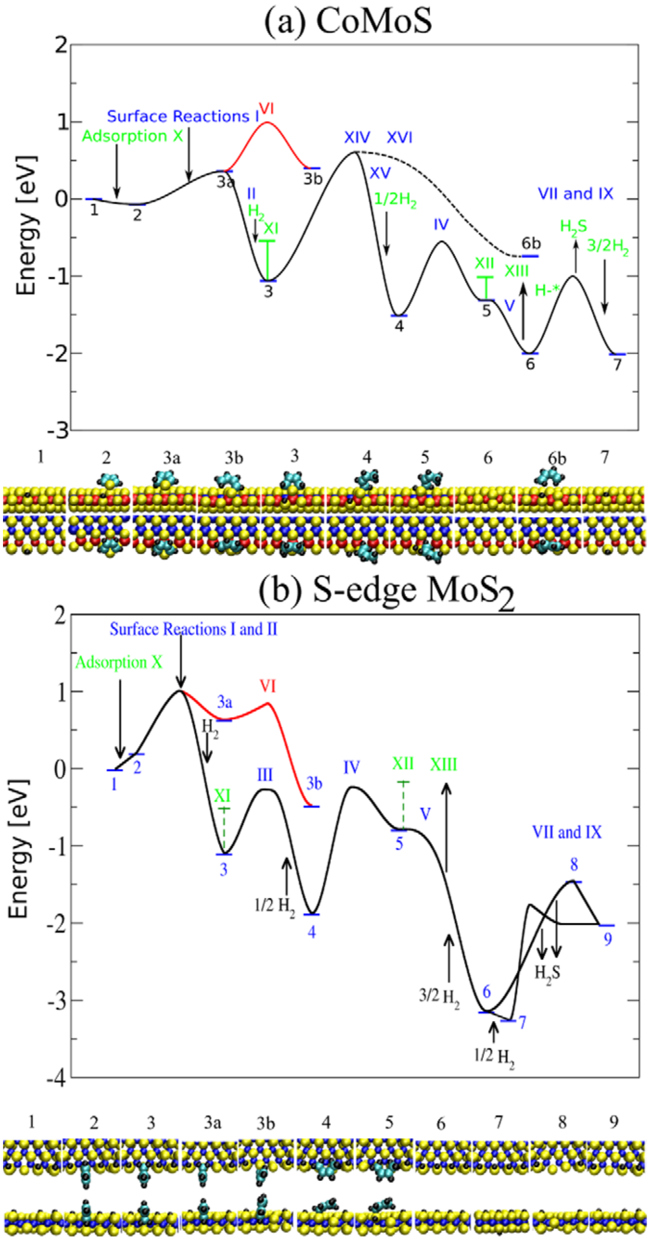

Fig. 2. (a) The S $(\bar{1}010)$ Co–Mo–S edge HYD and DDS pathway. The reference energy is chosen as the equilibrium edge configuration at HDS conditions (S-edge with 50% S and 25% H) and thiophene in the gas phase. The atoms are colored in the following color scheme: sulfur is yellow, molybdenum is blue, cobalt is red, carbon is cyan, and hydrogen is black. Arabic numerals denote intermediates: (1) the equilibrium structure, (2) thiophene, (3a) 2-hydro-thiophene-3-yl, (3b) *cis*-butadiene, (3) 2,5-dihydrothiophene, (4) *cis*-butenethiolate, (5) *cis*-butenethiol, (6) *cis*-butene in gas phase, (6b) *cis*-butadiene, (7) the equilibrium structure. Roman numerals refer to reaction numbers in Table 1. The DDS pathway is marked by the red line. The black line refers to the HYD pathway and the pathway leading to *cis*-butadiene is marked by a dotted black line. (b) The S $(\bar{1}010)$ edge of non-promoted MoS_2, adapted from Ref. [22]. The reference energy is chosen as a vacancy in the equilibrium edge configuration at HDS conditions and thiophene in the gas phase. Arabic numerals denote intermediates: (1) vacancy in the equilibrium structure with 75% H coverage, (2) thiophene, (3a) 2-hydro-thiophene-3-yl, (3b) *cis*-butadiene, (3) 2,5-dihydrothiophene, (4) *cis*-butenethiolate, (5) *cis*-butenethiol, (6) the equilibrium structure, (7) 125% H coverage, (8) vacancy with 50% H coverage, (9) vacancy with 75% H coverage. Roman numerals refer to reactions numbers in Table 1 of Ref. [22] which has the same numbering as Table 1. The DDS pathway is marked by the red line. (For interpretation of the references in colour in this figure legend, the reader is referred to the web version of this article.)

3.3. DDS pathway

The DDS pathway shown in Fig. 2a is initiated by thiophene adsorption (reaction X in Table 1). The weakly bound thiophene (−0.1 eV) reacts further by addition of an hydrogen atom to carbon 2 to form 2-hydro-thiophene-3-yl (reaction I in Table 1) with a barrier of 0.4 eV, equal to the energy change of the reaction. The C–S bond between S and the hydrogenated C in 2-hydro-thiophene-3-yl is broken without further hydrogenation forming *cis*-butadienethiolate with a barrier of 0.6 eV (reaction VI in Table 1). The final C–S-scission in the DDS pathway is assumed to take place in the same way as the final C–S-scission in the HYD pathway. The low hydrogenation barrier combined with the relatively low C–S-scission barrier indicates that the DDS pathway plays a major role at the Co–Mo–S brim site.

3.4. Hydrogenation and C–S-scission

In the case of non-promoted MoS_2, we concluded that hydrogenation primarily takes place at the Mo-edge due to the stronger binding of thiophene and the lower barrier at the Mo-edge compared to the S-edge [22]. Co-promotion of the S-edge increases the thiophene binding energy from 0.2 to −0.1 eV (see Fig. 2b). This is quite similar to the binding energy at the Mo-edge brim site which is also −0.1 eV. At the same time, the reaction barrier of 0.4 eV on the Co–Mo–S site is lower than the Mo-edge brim site barrier of 0.6 eV. The lower barrier could stem from the less tightly bound H atoms on Co–Mo–S, which are bound with 0.2 eV compared to 0.3 eV on the Mo-edge. Promoting MoS_2 with Co seems to increase the hydrogenation properties, an effect which also has been observed experimentally [9,10]. The Co–Mo–S edge is similar to the MoS_2 Mo-edge in the sense that it is an open structure where adsorption of large molecules such as 4,6-DMDBT are not sterically hindered. One might speculate that this is the reason why the Co–Mo–S edge is well suited for HDS of sterically hindered molecules for which the HYD pathway is important.

Co-promotion also influences the barriers of C–S-scission reactions. The C–S-scission of 2-hydro-thiophene-3-yl is the initial C–S-scission reaction in the DDS pathway. Its barrier of 1.1 eV is lower than the corresponding initial C–S-scission in the HYD pathway (C–S-scission of 2,5-dihydrothiophene). Compared to the non-promoted MoS_2 S-edge (see Fig. 2b) both C–S-scission reactions at the Co–Mo–S brim site have higher barriers than those at the unpromoted S-edge vacancy site [22,23].

It is interesting that both the HYD and DDS pathways may lead to butadiene as a product, since butadiene has been speculated to be an important product [53–56], but only observed experimentally in trace amounts [57]. Thus, the present results substantiate that butadiene is a product in HDS of thiophene.

3.5. Discussion

From the preceding sections, it is evident that Co-promotion of the S-edge changes the catalytic properties of this edge significantly. This is not surprising, as it is well known that the Co–Mo–S phase has a considerable higher activity than the unpromoted MoS_2 phase. In the following, we use the present results to qualitatively explain the origin of the main differences in reactivity. In general, we find that the Co–Mo–S edge has lower barriers for hydrogenation steps than non-promoted MoS_2 Mo- and S-edges (see Fig. 2b). Furthermore, the Co–Mo–S edge has lower barriers for C–S-scission steps compared to the non-promoted Mo-edge. This makes it relevant to compare the Co–Mo–S edge to both the Mo-edge and the S-edge of the unpromoted catalyst. The main observations are

- Adsorption of thiophene on Co–Mo–S $(\bar{1}010)$ is exothermic and similar to that on the unpromoted Mo-edge. This is in strong contrast to the unpromoted S-edge, at which adsorption of thiophene is endothermic.
- For the HYD pathway, the hydrogenation barrier (reaction I) and the C–S-scission barrier after hydrogenation (reaction III) are lower than those for the unpromoted Mo-edge. Compared to the unpromoted S-edge, the hydrogenation barrier (reaction I) is lower, but the C–S-scission barrier (reaction III) is higher.
- For the DDS pathway, thiophene adsorption is stronger, the hydrogenation barrier of thiophene is lower, and the C–S-scission barrier (reaction VI, 0.63 eV) is higher than that for the unpromoted S-edge (0.21 eV), but still rather modest resulting in a moderate overall barrier for the DDS pathway.
- All intermediates adsorb as strong or stronger than on the unpromoted Mo-edge.
- We previously established that on the unpromoted catalyst, the DDS reaction primarily takes place on the S-edge, which requires creation of a vacancy at the beginning of the catalytic cycle. The DDS pathway at the Co–Mo–S edge does not require vacancy creation, since vacancies are already present in the equilibrium structure. The S removal at the end of the catalytic cycle, which regenerates the active (equilibrium) structure, has a lower barrier than the initial vacancy creation of the unpromoted S-edge.

Comparing the HYD path to the DDS path at the Co–Mo–S edge, it is likely that the DDS path will dominate, as the DDS C–S-scission barrier (reaction VI) is lower than the HYD C–S-scission barrier (reaction III).

If we compare the Co–Mo–S edge to the unpromoted S-edge (see Fig. 2b and Table 1), there is a fundamental difference in how the reaction is initiated. On the unpromoted S-edge, a sulfur vacancy needs to be created in the first step, whereas on the Co–Mo–S edge, CUS sites are already present in the equilibrium structure. At these sites, HDS can take place without the removal of sulfur in the first step.

It is important to note that the present mechanism is completely different from previously proposed vacancy mechanisms [1]. This is in part related to the fact that until recently, not much was known about the exact structures of the different MoS_2 and Co–Mo–S edges. In the absence of such knowledge, the edge structures were assumed to have sulfurs in bulk-like positions, and the active sites were proposed to be vacancies derived from removing some of these sulfur atoms [1]. For the Mo-edge, it was often assumed that two of the sulfurs (the singly bonded ones) were easy to remove and under reaction conditions this edge was therefore proposed to contain two sulfur vacancies. Clearly, the present mechanism is very different from that imagined in previous vacancy mechanisms. Furthermore, the sulfur addition sites found in this study are also very different from vacancies or CUS sites proposed previously. In order to accommodate the present type mechanism one may choose to widen the concept of CUS sites such that a CUS site is a site at which HDS can take place without preceding removal of sulfur.

Taking a closer look at sulfur addition sites in the MoS_2 Mo-edge and Co–Mo–S, one may note that previous calculations [19] also determined the equilibrium structures under much higher chemical potential of sulfur (e.g. higher H_2S/H_2 pressure ratio) than that encountered under typical reaction conditions. At such conditions the sulfur coverage is higher, but the exact position of sulfur is not the same as for adsorbed thiophene in the present study. This is due to the involvement of the brim sites in the binding of thiophene.

Due to the presence of such CUS sites at the Co–Mo–S edge, we expect DDS to be enhanced by Co-promotion. Furthermore, adsorption and prehydrogenation of thiophene seems to be more favorable on Co–Mo–S due to the exothermic adsorption energy and low hydrogenation barrier (see Fig. 2a and Table 1). Finally, the regeneration of the active site has a modest barrier (1.0 eV), lower than the barrier for vacancy creation at the unpromoted S-edge. Thus, we find that Co promotes the DDS pathway and this agrees well with the previous experimental studies [10,9,15]. It should be stressed that the relatively low barrier for active site regeneration suggests that it is related to weaker binding of S. This agrees well with the early DFT studies by Byskov et al. as well as later studies and explains the less severe H_2S inhibition for Co–Mo–S compared to non-promoted MoS_2 which has been observed experimentally [1,9].

Considering the HYD pathway, we find that the hydrogenation activity should increase for the Co-promoted catalyst, since hydrogenation barriers are generally observed to be lower than those for unpromoted MoS_2. The C–S-scission barrier after initial hydrogenation (reaction III) for Co–Mo–S is also lower than that for the unpromoted Mo-edge, but higher than that for the unpromoted S-edge. It is possible to quantitatively predict the exact consequences of this by the construction of a microkinetic model and this is left to future studies. However, one can still conclude on a qualitative basis that also the HYD pathway seems to be important for the Co–Mo–S structure. The increased hydrogenation activity of Co–Mo–S compared to the non-promoted S-edge can possibly be attributed to the weaker H binding on Co–Mo–S which makes reactive H atoms available. The change in reactivity could be speculated to be a result of differences in the electronic structure of Co–Mo–S and non-promoted MoS_2. Earlier studies have found that the electronic structure of MoS_2 and Co–Mo–S is different [4,5], substantiated by more recent combined STM and DFT work [7]. Furthermore, recent studies have found a correlation between S and SH adsorption energies [61]. Even though these correlations are less well understood than similar correlations on transitions metals [62], it is intriguing that such similar correlations exist and understanding the underlying physics governing such correlations could be key to understanding the reactivity trends for sulfides.

In Ref. [22], it was discussed that not all the steps in a cycle for a pathway necessarily have to exclusively take place on a particular edge, but that intermediates may diffuse from one edge to the other. This may also be the case for Co–Mo–S, because the adsorption energies of the intermediates are more exothermic at the Co–Mo–S edge than on coexisting (unpromoted) Mo-edge. Thus, there is a thermodynamic driving force for the intermediates to move from the Mo-edge to the Co–Mo–S edge. For example, 2,5-dihydrothiophene adsorbs stronger on Co–Mo–S than on the unpromoted Mo-edge. Some amount of unpromoted Mo-edges exist on Co-promoted catalysts and these edges are likely to be active in hydrogenation of thiophene. Therefore, both edges may be involved in the same reaction cycle; for instance one might imagine a mechanism in which 2,5-dihydrothiophene produced at the Mo-edge subsequently undergoes C–S-scission at the Co–Mo–S edge.

In the literature, there has been a lot of speculation on the role of corner sites and a key issue has also been the role of stacking. However, the lack of detailed mechanistic studies has long hindered any specific conclusions regarding these important issues. However, with the present mechanistic insight one can start to address these issues in more detail. In previous STM experiments on thiophene hydrogenation and C–S bond breaking to thiolates, the resulting thiolate molecules have been observed to be very mobile and diffuse rapidly along the edges [27]. Therefore, one may presume that thiolates and other intermediates easily can diffuse to corner sites. The chemistry of corner sites has been found to be different from edge sites [59,60] and thus corner sites could play a different role than edge sites. In stacked multislab structures, one could also imagine that intermediates can desorb from one slab and readsorb on the neighboring slab. Furthermore, some adsorbates, especially large ones, will experience steric hindrances accessing the sites in stacked structures, and only the top layer can easily accommodate molecules requiring interaction with brim sites. These aspects will be a topic for future research.

4. Conclusion

Co-promotion of MoS_2 catalysts leads to the formation of the Co–Mo–S phase, in which Co atoms are incorporated into the $(\bar{1}010)$ S-edges of MoS_2 particles, forming the Co–Mo–S edge and significantly changing both the catalytic and structural properties of the catalyst [2,7,58]. An important consequence of Co-promotion is that the resulting Co–Mo–S equilibrium structure contains sulfur vacancies, i.e., that no additional sulfur vacancies need to be formed at the start of the catalytic cycle. This is in contrast to the unpromoted S-edge, which in its equilibrium state has full S coordination and therefore requires the creation of vacancies

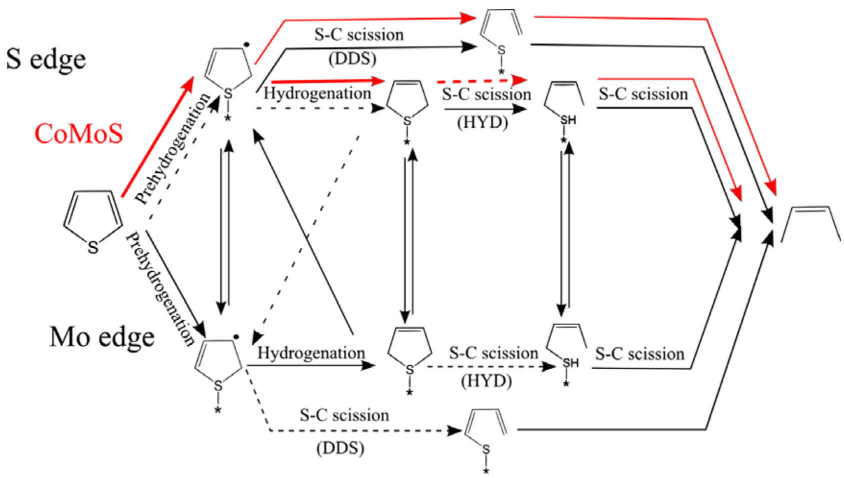

Fig. 3. Schematic overview over the reactions and structures involved in the HDS of thiophene, adapted from Refs. [22,23]. The atomic structures show the equilibrium structures at HDS conditions of the $(\bar{1}010)$ and the $(10\bar{1}0)$ edge. The schematic overview includes the reactions at the Co-promoted $(\bar{1}010)$ edge marked with red lines and the non-promoted $(\bar{1}010)$ edge marked with black lines in the upper part of the schematic and in the lower part the reactions at the non-promoted $(10\bar{1}0)$ edge [22,23] and in the middle the possible interactions between the two coexisting edges. The dotted arrows denote reactions found to be slow. (For interpretation of the references in colour in this figure legend, the reader is referred to the web version of this article.)

as the first step in a catalytic cycle. At the Co–Mo–S edge, special CUS sites are present under equilibrium conditions and the catalysis does not require vacancy formation in the first step. This is very different from the catalysis occurring at unpromoted S-edges and the new insight stresses that it is important to consider that HDS reactions can occur both via initial vacancy creation and via sulfur addition. The Co–Mo–S active sites exhibit a bright brim [7,8] analogues to the Mo-edge brim site.

Turning to the catalytic activity, Fig. 3 gives a schematic overview of the reaction pathways for thiophene HDS over a Co–Mo–S catalyst and over the unpromoted MoS_2 catalyst for comparison. The main effect of the Co-promotion is to make the Co–Mo–S edge suitable for both hydrogenation and C–S-scission steps, whereas the unpromoted Mo- and S-edges are primarily suited for one of the two. There is a thermodynamic driving force for adsorbed intermediates to move from the (unpromoted) Mo-edge to the Co–Mo–S edge and therefore hydrogenation may take place at both the Mo-edge and the Co–Mo–S edge. The overall conclusion is that Co-promotion increases the hydrogenation properties of the catalyst. For Co–Mo–S, the C–S-scission barriers are higher than those for the non-promoted S-edge but lower than those for the non-promoted Mo-edge. However, due to the increased hydrogenation activity and increased adsorption energy of thiophene, we expect the activity of the Co–Mo–S brim site to be higher than the one of the unpromoted S-edge for the DDS pathway.

Acknowledgments

The Center for Atomic-scale Materials Design is sponsored by the Lundbeck Foundation. The Danish Center for Scientific Computing is acknowledged for granting the computer resources needed for this project.

Appendix A. Supplementary material

Supplementary data associated with this article can be found, in the online version, at doi:10.1016/j.jcat.2009.09.016.

References

[1] H. Topsøe, B.S. Clausen, F.E. Massoth, Hydrotreating Catalysis, Science and Technology, Springer-Verlag, Berlin, 1996.

[2] H. Topsøe, R. Candia, N.Y. Topsøe, B.S. Clausen, On the state of the Co–Mo–S Model, Bulletin des Sociétés Chimiques Belges 93 (8–9) (1984) 783–806.

[3] L.S. Byskov, B. Hammer, J.K. Nørskov, B.S. Clausen, H. Topsøe, Sulfur bonding in MoS_2 and Co–Mo–S structures, Catalysis Letters 47 (1997) 177–182.

[4] L.S. Byskov, J.K. Nørskov, B.S. Clausen, H. Topsøe, DFT calculations of unpromoted and promoted MoS_2-based hydrodesulfurization catalysts, Journal of Catalysis 187 (1999) 109–122.

[5] P. Raybaud, J. Hafner, G. Kresse, S. Kasztelan, H. Toulhoat, Structure, energetics, and electronic properties of the surface of a promoted MoS_2 catalyst: an ab initio local density functional study, Journal of Catalysis 190 (2000) 128–143.

[6] H. Schweiger, P. Raybaud, H. Toulhoat, Promoter sensitive shapes of Co(Ni)MoS nanocatalysts in sulfo-reductive conditions, Journal of Catalysis 212 (2002) 33–38.

[7] J.V. Lauritsen, J. Kibsgaard, G.H. Olesen, P.G. Moses, B. Hinnemann, S. Helveg, J.K. Nørskov, B.S. Clausen, H. Topsøe, E. Lægsgaard, F. Besenbacher, Location and coordination of promotor atoms in Co- and Ni-promoted MoS_2- based hydrotreating catalysts, Journal of Catalysis 249 (2007) 220–233.

[8] J.V. Lauritsen, S. Helveg, E. Lægsgaard, I. Stensgaard, B.S. Clausen, H. Topsøe, F. Besenbacher, Atomic-scale structure of Co–Mo–S nanoclusters in hydrotreating catalysts, Journal of Catalysis 197 (2001) 1–5.

[9] M. Egorova, R. Prins, Hydrodesulfurization of dibenzothiophene and 4,6-dimethyldibenzothiophene over sulfided NiMo/γ-Al_2O_3, CoMo/γ-Al_2O_3, and Mo/γ-Al_2O_3 catalysts, Journal of Catalysis 225 (2004) 417–427.

[10] F. Bataille, J.L. Lemberton, P. Michaud, G. Pérot, M. Vrinat, M. Lemaire, E. Schulz, M. Breysse, S. Kasztelan, Alkyldibenzothiophenes hydrodesulfurization-promoter effect, reactivity, and reaction mechanism, Journal of Catalysis 191 (2000) 409–422.

[11] D. Kasahara, T. Shimizu, M. Yamada, Inhibiting effects of H_2S on HDS activity of CoMo-, NiMo-, and Mo/Al_2O_3, Catalysis Today 35 (1997) 59–64.

[12] X.L. Ma, K. Sakanishi, T. Isoda, I. Mochida, Hydrodesulfurization reactivities of narrow-cut fractions in a gas oil, Industrial and Engineering Chemistry Research 34 (1995) 748–754.

[13] M.V. Landau, D. Berger, M. Herskowitz, Hydrodesulfurization of methyl-substituted dibenzothiophenes: fundamental study of routes to deep desulfurization, Journal Of Catalysis 159 (1996) 236–245.

[14] D.D. Whitehurst, H. Farag, T. Nagamatsu, K. Sakanishi, I. Mochida, Assessment of limitations and potentials for improvement in deep desulfurization through detailed kinetic analysis of mechanistic pathways, Catalysis Today 45 (1998) 299–305.

[15] B. Yoosuk, J.H. Kim, C. Song, C. Ngamcharussrivichai, P. Prasassarakich, Highly active MoS_2, $CoMoS_2$ and $NiMoS_2$ unsupported catalysts prepared by hydrothermal synthesis for hydrodesulfurization of 4,6-dimethyldibenzothiophene, Catalysis Today 130 (2008) 14–23.

[16] E. Lecrenay, K. Sakanishi, I. Mochida, T. Suzuka, Hydrodesulfurization activity of CoMo and NiMo catalysts supported on some acidic binary oxides, Applied Catalysis A: General 175 (1998) 237–243.

[17] J.K. Nørskov, B.S. Clausen, H. Topsøe, Understanding the trends in the hydrodesulfurization activity of the transition metal sulfides, Catalysis Letters 13 (1992) 1–8.

[18] P. Raybaud, J. Hafner, G. Kresse, S. Kasztelan, H. Toulhoat, Ab initio study of the H_2–H_2S/MoS_2 gas–solid interface: the nature of the catalytically active sites, Journal of Catalysis 189 (2000) 129–146.

[19] M.V. Bollinger, K.W. Jacobsen, J.K. Nørskov, Atomic and electronic structure of MoS_2 nanoparticles, Physical Review B 67 (2003) 085410.

[20] M. Sun, A.E. Nelson, J. Adjaye, On the incorporation of nickel and cobalt into MoS_2-edge structures, Journal of Catalysis 226 (2004) 32–40.

[21] S. Cristol, J.F. Paul, E. Payen, D. Bougeard, S. Clémendot, F. Hutschka, Theoretical study of the $MoS_2(100)$ surface: a chemical potential analysis of sulfur and hydrogen coverage, Journal of Physical Chemistry B 104 (2000) 11220–11229.

[22] P.G. Moses, B. Hinnemann, H. Topsøe, J.K. Nørskov, The hydrogenation and direct desulfurization reaction pathway in thiophene hydrodesulfurization over MoS_2 catalysts at realistic conditions: a density functional study, Journal of Catalysis 248 (2007) 188–203.

[23] P.G. Moses, B. Hinnemann, H. Topsøe, J.K. Nørskov, Corrigendum to the hydrogenation and direct desulfurization reaction pathway in thiophene hydrodesulfurization over MoS_2 catalysts at realistic conditions: a density functional study [J. Catal. 248 (2007) 188], Journal of Catalysis 260 (2008) 202–203.

[24] S. Helveg, J.V. Lauritsen, E. Lægsgaard, I. Stensgaard, J.K. Nørskov, B.S. Clausen, H. Topsøe, F. Besenbacher, Atomic-scale structure of single-layer MoS_2 nanoclusters, Physical Review Letters 84 (2000) 951–954.

[25] M.V. Bollinger, J.V. Lauritsen, K.W. Jacobsen, J.K. Nørskov, S. Helveg, F. Besenbacher, One-dimensional metallic edge states in MoS_2, Physical Review Letters 87 (2001) 196803.

[26] J.V. Lauritsen, M. Nyberg, R.T. Vang, M.V. Bollinger, B.S. Clausen, H. Topsøe, K.W. Jacobsen, E. Lægsgaard, J.K. Nørskov, F. Besenbacher, Chemistry of one-dimensional metallic edge states in MoS_2 nanoclusters, Nanotechnology 14 (2003) 385–389.

[27] J.V. Lauritsen, M. Nyberg, J.K. Nørskov, B.S. Clausen, H. Topsøe, E. Lægsgaard, F. Besenbacher, Hydrodesulfurization reaction pathways on MoS_2 nanoclusters revealed by scanning tunneling microscopy, Journal of Catalysis 224 (2004) 94–106.

[28] B. Hinnemann, J.K. Nørskov, H. Topsøe, A density functional study of the chemical differences between type I and type II MoS_2-based structures in hydrotreating catalysts, Journal of Physical Chemistry B 109 (2005) 2245–2253.

[29] E.J.M. Hensen, V.H.J. de Beer, J.A.R. van Veen, R.A. van Santen, A refinement on the notion of type I and II (Co)MoS phase in hydrotreating catalysts, Catalysis Letters 84 (2002) 59–67.

[30] R. Candia, O. Sørensen, J. Villadsen, N.Y. Topsøe, B.S. Clausen, H. Topsøe, Effect of sulfiding temperature on activity and structures of Co–Mo/Al_2O_3, catalysts. II, Bulletin des Sociétés Chimiques Belges 93 (1984) 763–773.

[31] N.Y. Topsøe, Infrared study of sulfided Co–Mo/Al_2O_3 catalysts: the nature of surface hydroxyl groups, Journal of Catalysis 64 (1980) 235–237.

[32] B. Hammer, L.B. Hansen, J.K. Nørskov, Improved adsorption energetics within density-functional theory using revised Perdew–Burke–Ernzerhof functionals, Physical Review B 59 (1999) 7413–7421.

[33] S.R. Bahn, K.W. Jacobsen, An object-oriented scripting interface to a legacy electronic structure code, Computing in Science and Engineering 4 (2002) 56–66.

[34] H.J. Monkhorst, J.D. Pack, Special points for Brillouin-zone integrations, Physical Review B 13 (1976) 5188–5192.

[35] Th. Böker, R. Severin, A. Müller, C. Janowitz, R. Manzke, D. Voss, P. Krüger, A. Mazur, J. Pollmann, Band structure of MoS_2, $MoSe_2$ and α-$MoTe_2$: angle resolved photoelectron spectroscopy and *ab initio* calculations, Physical Review B 64 (2001) 235305.

[36] K. Laasonen, A. Pasquarello, R. Car, C. Lee, D. Vanderbilt, Car–Parrinello molecular-dynamics with vanderbilt ultrasoft pseudopotentials, Physical Review B 47 (1993) 10142–10153.

[37] N. Troullier, J.L. Martins, Efficient pseudopotentials for plane-wave calculations, Physical Review B 43 (1991) 1993–2006.

[38] D. Vanderbilt, Soft self-consistent pseudopotentials in a generalized eigenvalue formalism, Physical Review B 41 (1990) 7892–7895.

[39] J.P. Perdew, J.A. Chevary, S.H. Vosko, K.A. Jackson, M.R. Pederson, D.J. Singh, C. Fiolhais, Atoms, molecules, solids, and surfaces: applications of the generalized

gradient approximation for exchange and correlation, Physical Review B 46 (1992) 6671–6687.

[40] H. Jónsson, G. Mills, K.W. Jacobsen, Nudged elastic band method for finding minimum energy paths of transitions, in: B.J. Berne, G. Cicotti, D.f. Coker (Eds.), Classical and Quantum Dynamics in Condensed Phase Simulations, World Scientific, Singapore, 1998.

[41] P. Maragakis, S.A. Andreev, Y. Brumer, D.R. Reichman, E. Kaxiras, Adaptive nudged elastic band approach for transition state calculation, Journal of Chemical Physics 117 (2002) 4651–4658.

[42] P. Culot, G. Dive, V.H. Nguyen, J.M. Ghuysen, A quasi-newton algorithm for first-order saddle-point location, Theoretica Chimica Acta 82 (1992) 189–205.

[43] W. Humphrey, A. Dalke, K. Schulten, VMD-Visual molecular dynamics, Journal of Molecular Graphics 14 (1996) 33–38.

[44] E. Krebs, B. Silvi, P. Raybaud, Mixed sites and promoter segregation: a DFT study of the manifestation of Le Chatelier's principle for the Co(Ni)MoS active phase in reaction conditions, Catalysis Today 130 (2008) 160–169.

[45] A.D. Gandubert, E. Krebs, C. Legens, D. Costa, D. Guillaume, P. Raybaud, Optimal promoter edge decoration of CoMoS catalysts: a combined theoretical and experimental study, Catalysis Today 130 (2008) 149–159.

[46] W. Niemann, B.S. Clausen, H. Topsøe, X-ray absorption studies of the Ni environment in Ni–Mo–S, Catalysis Letters 4 (1990) 355–364.

[47] S.M.A.M. Bouwens, J. Van Veen, D.C. Koningsberger, V.H.J. De Beer, R. Prins, Extended X-ray absorption fine-structure determination of the structure of cobalt in carbon-supported Co and Co–Mo sulfide hydrodesulfurization catalysts, Journal of Physical Chemistry 95 (1991) 123–134.

[48] J.F. Paul, S. Cristol, E. Payen, Computational studies of (mixed) sulfide hydrotreating catalysts, Catalysis Today 130 (2008) 139–148.

[49] M.L. Vrinat, The kinetics of the hydrodesulfurization process – a review, Applied Catalysis 6 (1983) 137–158.

[50] M. Dion, H. Rydberg, E. Schröder, D.C. Langreth, B.I. Lundqvist, Van der Waals density functional for general geometries, Physical Review Letters 92 (2004) 246401.

[51] J.J. Mortensen, L.B. Hansen, K.W. Jacobsen, Real-space grid implementation of the projector augmented wave method, Physical Review B 71 (2005) 035109.

[52] P.G. Moses, J.J. Mortensen, B.I. Lundqvist, J.K. Nørskov, Density functional study of the adsorption and van der Waals binding of aromatic and conjugated compounds on the basal plane of MoS_2, Journal of Chemical Physics 130 (2009) 104709.

[53] A. Borgna, E.J.M. Hensen, J.A.R. van Veen, J.W. Niemantsverdriet, Intrinsic kinetics of thiophene hydrodesulfurization on a sulfided $NiMo/SiO_2$ planar model catalyst, Journal of Catalysis 221 (2004) 541–548.

[54] P.J. Owens, C.H. Amberg, Thiophene desulfurization by a microreactor technique, Advances in Chemistry 33 (1961) 182–198.

[55] A.E. Hargreaves, J.R.H. Ross, An investigation of the mechanism of the hydrodesulfurization of thiophene over sulfided $Co–Mo/Al_2O_3$ catalysts II. The effect of promotion by cobalt on the C–S bond cleavage and double-bond hydrogenation/dehydrogenation activities of tetrahydrothiophene and related compounds, Journal of Catalysis 56 (1979) 363–376.

[56] K.F. McCarty, G.L. Schrader, Deuterodesulfurization of thiophene: An investigation of the reaction-mechanism, Journal of Catalysis 103 (1987) 261–269.

[57] D.L. Sullivan, J.G. Ekerdt, Mechanisms of thiophene hydrodesulfurization on model molybdenum catalysts, Journal of Catalysis 178 (1998) 226–233.

[58] F. Besenbacher, M. Brorson, B.S. Clausen, S. Helveg, B. Hinnemann, J. Kibsgaard, J. Lauritsen, P.G. Moses, J.K. Nørskov, H. Topsøe, Recent STM, DFT and HAADF-STEM studies of sulfide-based hydrotreating catalysts: insight into mechanistic, structural and particle size effects, Catalysis Today 130 (2008) 86–96.

[59] R. Koide, E.J.M. Hensen, J.F. Paul, S. Sylvain, E. Payen, H. Nakamura, R.A. van Santen, A DFT study on benzene adsorption over a corner site of tungsten sulfides, Catalysis Today 130 (2008) 178–182.

[60] L.S. Byskov, J.K. Nørskov, B.S. Clausen, H. Topsøe, Edge termination of MoS_2 and CoMos catalyst particles, Catalysis Letters 64 (2000) 95–99.

[61] E.M. Fernández, P.G. Moses, A. Toftelund, H.A. Hansen, J.I. Martinez, F. Abild-Pedersen, J. Kleis, B. Hinnemann, J. Rossmeisl, T. Bligaard, J.K. Nørskov, Scaling relationships for adsorption energies on transition metal oxide, sulfide, and nitride surfaces, Angewandte Chemie – International Edition 47 (2008) 4683–4686.

[62] F. Abild-Pedersen, J. Greeley, F. Studt, J. Rossmeisl, T.R. Munter, P.G. Moses, E. Skulason, T. Bligaard, J.K. Nørskov, Scaling properties of adsorption energies for hydrogen-containing molecules on transition-metal surfaces, Physical Review Letters 99 (2007) 016105.